Biochemical Journal (2023) **480** 1097–1107
https://doi.org/10.1042/BCJ20230139

PORTLAND PRESS

Research Article

Computational design of Matrix Metalloproteinase-9 (MMP-9) resistant to auto-cleavage

Alessandro Bonadio[1,*], Solomon Oguche[1,*], Tali Lavy[2], Oded Kleifeld[2] and Julia Shifman[1]

[1]Department of Biological Chemistry, The Alexander Silberman Institute of Life Sciences, The Hebrew University of Jerusalem, Jerusalem, Israel; [2]Faculty of Biology, Technion-Israel Institute of Technology, Haifa, Israel

Correspondence: Julia Shifman (jshifman@mail.huji.ac.il)

Matrix metalloproteinase-9 (MMP-9) is an endopeptidase that remodels the extracellular matrix. MMP-9 has been implicated in several diseases including neurodegeneration, arthritis, cardiovascular diseases, fibrosis and several types of cancer, resulting in a high demand for MMP-9 inhibitors for therapeutic purposes. For such drug design efforts, large amounts of MMP-9 are required. Yet, the catalytic domain of MMP-9 ($MMP\text{-}9_{Cat}$) is an intrinsically unstable enzyme that tends to auto-cleave within minutes, making it difficult to use in drug design experiments and other biophysical studies. We set our goal to design $MMP\text{-}9_{Cat}$ variant that is active but stable to auto-cleavage. For this purpose, we first identified potential auto-cleavage sites on $MMP\text{-}9_{Cat}$ using mass spectroscopy and then eliminated the auto-cleavage site by predicting mutations that minimize auto-cleavage potential without reducing enzyme stability. Four computationally designed $MMP\text{-}9_{Cat}$ variants were experimentally constructed and evaluated for auto-cleavage and enzyme activity. Our best variant, Des2, with 2 mutations, was as active as the wild-type enzyme but did not exhibit auto-cleavage after 7 days of incubation at 37°C. This $MMP\text{-}9_{Cat}$ variant, with an identical with $MMP\text{-}9_{Cat}$ WT active site, is an ideal candidate for drug design experiments targeting MMP-9 and enzyme crystallization experiments. The developed strategy for $MMP\text{-}9_{CAT}$ stabilization could be applied to redesign other proteases to improve their stability for various biotechnological applications.

Introduction

Matrix metalloproteinases (MMPs) are a family of proteases, comprising more than twenty different enzymes in humans. They are composed of a catalytic domain with a catalytic zinc ion, a pro-domain which is cleaved off upon enzyme activation by MMPs and other proteases [1,2], an optional transmembrane domain, and additional domains utilized in the substrate and other proteins binding [3]. MMPs are involved in multiple biological processes, including remodeling of the extracellular matrix (ECM), shedding of cell surface receptors and membrane-bound signaling molecules, angiogenesis, intravasation/extravasation from blood vessels, and immune cells maturation [4]. Dysregulation and overexpression of some of the MMPs family members affect these processes leading to many pathological conditions such as neurodegeneration, arthritis, cardiovascular diseases, fibrosis, and cancer [5]. It is not surprising that MMPs play an important role in cancer metastasis, with multiple MMPs overexpressed in solid tumors [4,6–10]. Due to the important role of MMPs in cancer, there has been considerable effort to develop MMP inhibitors, from zinc chelators [11–13] to antibodies [14–18]. In particular, several drug design efforts have been directed against matrix metalloproteinase-9 (MMP-9) as it is an established target in several types of cancer, inflammation, and cardiac and neurodegenerative diseases [19]. A monoclonal antibody Andecaliximab directed against MMP-9 is being evaluated in multiple phase 3 clinical trials involving solid tumors [16,17]. We and others have engineered potent and selective inhibitors of MMP-9 starting from the endogenous MMP inhibitor N-TIMP2 [20–24].

*These authors contributed equally to this work.

Received: 11 April 2023
Revised: 22 June 2023
Accepted: 3 July 2023

Accepted Manuscript online: 4 July 2023
Version of Record published: 17 July 2023

Biochemical Journal (2023) 480 1097–1107
https://doi.org/10.1042/BCJ20230139

Drug design efforts targeting MMP-9 require large amounts of the enzyme being produced. However, working with MMP-9 has been challenging due to enzyme instability. Indeed, all routine procedures such as protein labeling, dialysis, crystallization, and other experiments requiring long incubations and high protein concentrations are extremely challenging with this enzyme due to the fast loss of the active protein. The major reason for this loss is the capability of MMP-9 to auto-degrade; self-cleavage becomes more prominent at higher protein concentrations [25,26]. To obviate the problem, weak MMP inhibitors such as acetohydroxamic acid (AHA) have been used in MMP-9 purification procedures. However, the inhibitor has to be removed prior to further experiments and upon removal, the self-cleavage problem returns [27]. To alleviate self-cleavage and improve MMP-9 stability, MMP-9 mutants that remove the catalytic Glu and abolish catalytic activity, E402Q and E402A, have been utilized in some studies [27,28]. Such enzyme variants are more stable but present a modified active site, with the negative charge of E402 removed. Thus, these active-site MMP-9 mutants could not be used in MMP-9 drug design or screening experiments.

In the current study, we present a novel approach for engineering the active catalytic domain of MMP-9 ($MMP\text{-}9_{Cat}$) variants that are resistant to self-cleavage by identifying and removing the self-cleavage site from the enzyme sequence. Using the computational design, we introduce a minimum number of mutations that preserve protein structure and activity but decrease the probability of sequence cleavage by MMP-9. Our best design with two mutations 10 Å away from the active site does not auto-cleave after seven days of incubation at 37°C while retaining WT-like MMP-9 activity.

Results

Design of the non-degrading MMP-9 variants

For our studies, we utilized the MMP-9 construct that contained only the MMP-9 catalytic domain construct referred to as $MMP\text{-}9_{Cat}$ (residues 107–215 fused to 391–443) with the hemopexin-like and fibronectin type II domains truncated [28]. We have been routinely expressing $MMP\text{-}9_{Cat}$ in *Escherichia coli* [22], refolding the enzyme from inclusion bodies, and performing subsequent purification with size exclusion chromatography (SEC). While this protocol always yielded active protein, more than 90% of the protein was lost during refolding and purification. The loss of active $MMP\text{-}9_{Cat}$ WT was at least partially due to the fast self-cleavage of the enzyme, as could be observed on the SDS–PAGE gel analysis of the pure $MMP\text{-}9_{Cat}$ WT sample (Figure 1A).

To identify the $MMP\text{-}9_{Cat}$ WT auto-cleavage site(s), we extracted the early auto-cleavage product (Band B1 on the gel), digested it with trypsin, and performed the liquid chromatography with tandem mass spectroscopy (LC–MS/MS) analysis (Supplementary data). Our data analysis aimed at the identification of semi-tryptic

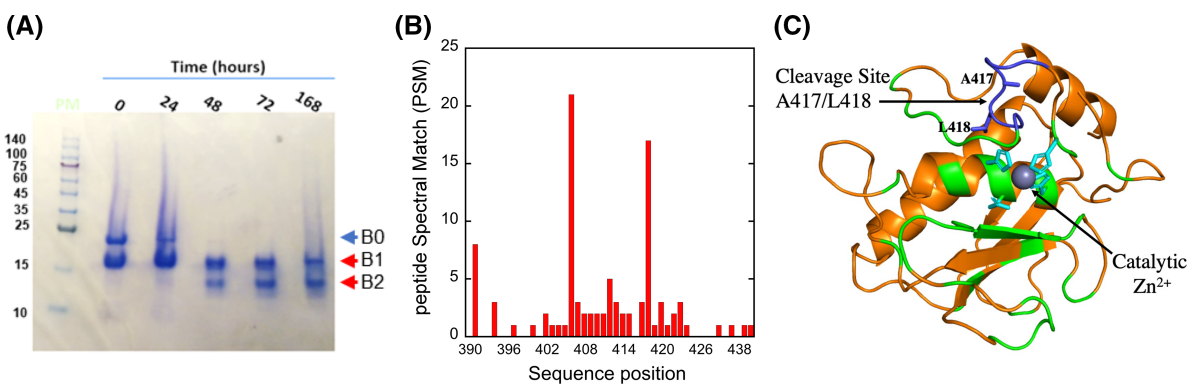

Figure 1. MMP-9 auto-degradation site is a partially exposed loop.

(**A**) SDS–PAGE gel analysis of $MMP\text{-}9_{Cat}$ WT at 25°C showing the full-length (blue arrow) and degradation products (red arrows). (**B**) The relative auto-cleavage preference of $MMP\text{-}9_{Cat}$ WT. Cleavage preference was calculated from the LS/MS count of each peptide product contributing to a given cleavage site at a specific sequence position. The *X*-axis represents the amino acid residue number of the full MMP-9 sequence. The C-terminal cleavage positions with the highest peptide spectral match (PSM) were after positions 405 and 417. (**C**) Structure of $MMP\text{-}9_{Cat}$ WT (orange) in cartoon representation, showing the catalytic Zn^{2+} and the predicted auto-cleavage site in the partially exposed loop (colored in blue). Amino acids at the interface with the MMP protein inhibitor TIMP-2 are colored in green. Zn^{2+} ligating residues are colored in cyan.

peptides whose non-tryptic termini were generated due to MMP-9_{Cat} self-cleavage. This analysis showed four possible cleavage sites: the N-terminal sites with P1 positions 185 and 190 and the C-terminal sites with P1 positions 405 and 417 on MMP-9_{Cat} WT (Figure 1B). Only the C-terminal cleavage sites, however, were consistent with the cleavage product of 16 kDa observed by SDS–PAGE (B1 on Figure 1A). Among the two identified C-terminal cleavage sites, the cleavage site between positions A417 and L418 on MMP-9_{Cat} WT had been identified in a previous study that analyzed the MMP-9 self-cleavage profile [26]. Inspection of the A417/L418 self-cleavage site revealed that it is 10 Å away from the active site and away from the MMP-9 binding interface with the broad MMP protein inhibitor TIMP-2 and small molecule MMP inhibitors (Figure 1C). We hence decided that the A417/L418 is the most promising site for redesign with the goal of eliminating MMP-9_{Cat} WT auto-cleavage activity.

We set our goal to design a stable to auto-cleavage MMP-9_{Cat} variant by introducing mutations in the auto-cleavage site that reduce the MMP-9_{Cat} auto-cleavage score but at the same time do not destabilize the enzyme. We wanted to introduce a minimal number of mutations in order to keep the MMP-9_{Cat} sequence and structure as similar to WT as possible, preserving the active site and the binding interface with a broad MMP family inhibitor TIMP-2. We hence considered four amino acids before and after the identified cleavage site, as commonly done in the analysis of protease substrate specificity [29]. We then ran a single-position mutational scan of these eight MMP-9_{Cat} positions and calculated the auto-cleavage score using the Procleave web server [30]. At the same time, protein stability of all single mutants was predicted using Rosetta FastDesign [31], thus generating both self-cleavage probability matrix and stability matrix for all possible positions at these eight MMP-9_{Cat} residues (Figure 2A,B).

We then compared the computational scans for auto-degradation and stability and the multiple sequence alignments of MMPs for those eight positions and selected mutations that improved self-cleavage score without compromising stability (Figure 2C). Comparing the design models to the structure of the homologs, we further selected designs that recapitulated homologous structures, both at the mutated positions and its structural neighbors, producing Des1 and Des2 (Figure 2D). A few additional mutations were introduced with RosettaFast design at other MMP-9_{Cat} positions to stabilize the designs further, producing Des3 and Des4 sequences. Thus, four MMP-9_{Cat} designs targeting different positions were selected for experimental characterization (Table 1).

Experimental characterization of the designed MMP-9_{Cat} variants

The MMP-9_{Cat} WT and four variants (Des1, Des2, Des3, and Des4) were expressed in *E. coli* BL21. The expression yield of the designed variants was comparable with that of MMP-9_{Cat} WT (Supplementary Figure S2). The expressed proteins were refolded on a nickel NTA column and purified by anion exchange (AIEX) chromatography (Supplementary Figure S3A). All protein variants expressed and refolded in quantities similar to that of MMP-9_{Cat} WT and eluted at similar times.

Designs were tested for their ability to cleave a peptide with an optimal MMP-9 recognition sequence. Such experiments were performed using an enzyme activity assay that measures the cleavage of a fluorogenic substrate peptide, resulting in fluorescence at 395 nm [32]. All four designs showed activity comparable to MMP-9_{Cat} WT, indicating that they were properly folded (data not shown). We next evaluated whether our variants were stable to self-cleavage by analyzing them with SDS–PAGE immediately after purification with AIEX. Gel electrophoresis analysis showed that Des1, Des3, and Des4 exhibited partial self-cleavage immediately after purification similar to that of MMP-9_{Cat} WT while Des2 did not exhibit self-cleavage (Supplementary Figure S2B). We hence selected Des2 for further evaluation.

To quantitatively compare the enzymatic parameters of Des2 and MMP-9_{Cat} WT, we measured the proteolysis reaction rate at increasing concentrations of the fluorogenic substrate peptide and determined K_m and k_{cat} values for the two enzyme variants. Our data show that K_m, k_{cat}, and k_{cat}/K_m for Des2 were very similar to those exhibited by MMP-9_{Cat} WT, demonstrating that enzyme kinetics and the catalytic efficiency of the protein is not affected by the two introduced mutations (Supplementary Figure S4 and Table 2). We next sought to compare the auto-cleavage activity of Des2 to that of MMP-9_{Cat} WT over a longer period of time. For this purpose, we incubated a 0.5 μM sample of Des2 and MMP-9_{Cat} WT at 37°C for a maximum of seven days and analyzed the samples on SDS–PAGE as time progressed (Figure 3A). Our data show that an auto-cleavage band appeared in the MMP-9_{Cat} WT sample already after 1 h of incubation and the protein degraded almost completely after 7 days (Figure 3A, top). In contrast, Des2 showed no auto-cleavage product even at the end of the 7-day period (Figure 3A, bottom).

Biochemical Journal (2023) 480 1097–1107
https://doi.org/10.1042/BCJ20230139

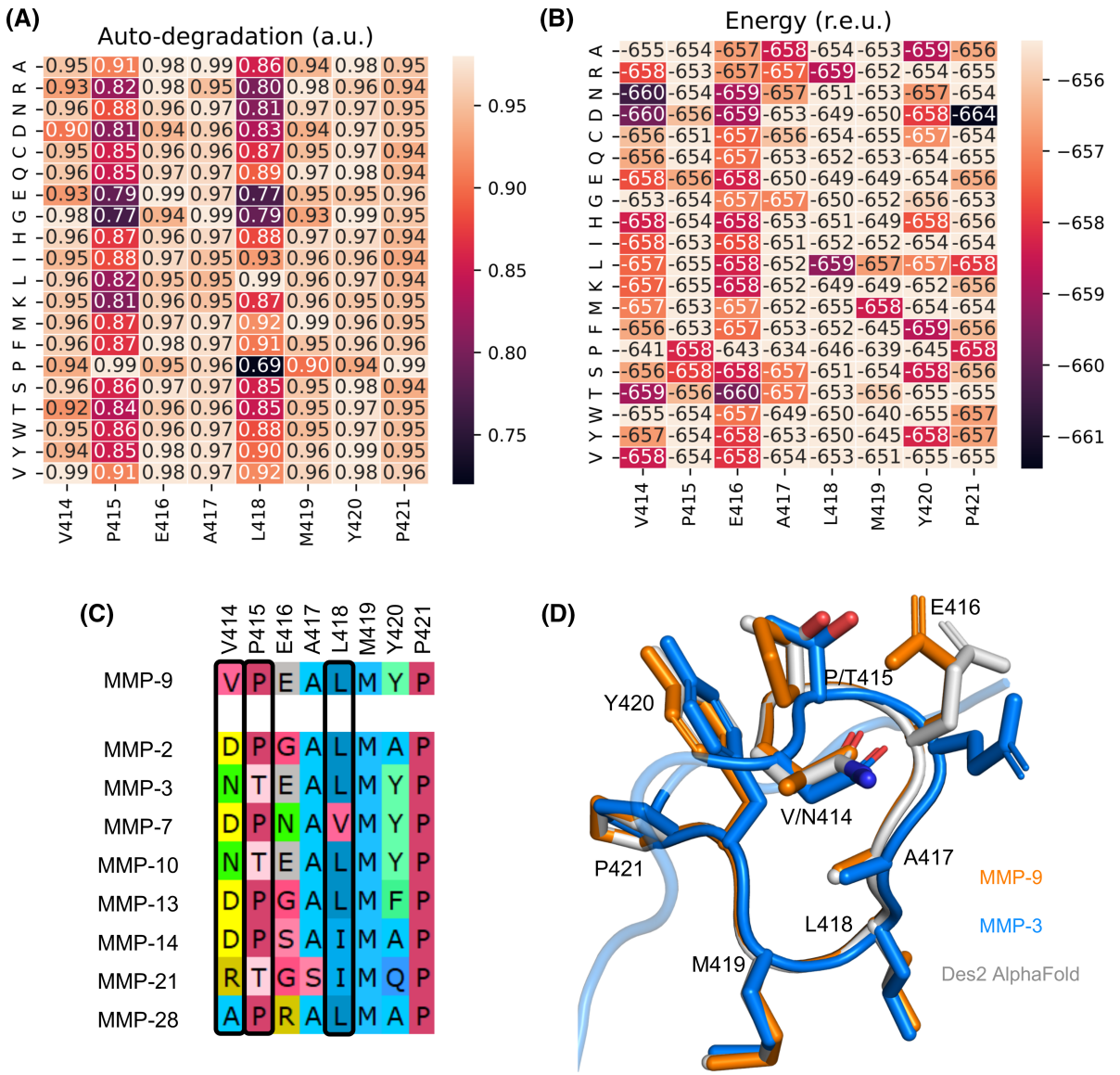

Figure 2. Design of non-degrading MMP-9$_{Cat}$ variants.

(**A**) Saturation mutagenesis scan of the cleavage loop displaying the auto-cleavage score according to the Procleave webserver [30]. (**B**) Saturation mutagenesis scan of the cleavage loop displaying the Rosetta energy. (**C**) Alignment of eight representative MMPs in the region of the predicted auto-cleavage site. Alignment of all 23 human MMPs is shown in Supplementary Figure S1. D414, N414, T415, and I418 are frequently present in MMP-9 homologs and confer lower predicted auto-cleavage scores compared with that of the MMP-9$_{Cat}$ WT sequence and exhibit favorable energy according to Rosetta. (**D**) A model of the Des2 loop according to AlphaFold (light gray) superimposed onto the structures of MMP-3 (blue, PDB: 4DP3) and MMP-9 (orange, PDB: 5TH9). The mutated N414 and T415 in Des2 have the same rotamers as in the homologous MMP-3 structure as well as the same neighboring amino acids and most of the same rotamers among neighboring positions, increasing the confidence in Des2 foldability.

We next measured the enzymatic activity of MMP-9$_{Cat}$ WT and Des2 at three time points ($T = 0$, $T = 3$d, and $T = 7$d) (Figure 3B). In agreement with the SDS–PAGE results, MMP-9$_{Cat}$ WT activity decreased with successive time points as more enzyme is cleaved, while Des2 maintained 100% activity at all time points. The same tendency was observed when evaluating the enzyme's inhibition by its strong active-site inhibitor, prinomastat (Figure 3C, Table 3). While the concentration of the active enzyme for MMP-9$_{Cat}$ WT decreased as

Biochemical Journal (2023) **480** 1097–1107
https://doi.org/10.1042/BCJ20230139

Table 1. The four design sequences with the predicted auto-cleavage and energy scores

	147	400	414	415	416	417	418	Auto-cleavage score (a.u)	Energy score (r.e.u.)
MMP-9_{Cat} WT	L	A	V	P	E	A	L	0.99	−658
Des1	—	—	D	—	—	—	—	0.90	−660
Des2	—	—	N	T	—	—	—	0.62	−657
Des3[1]	V	V	—	—	—	—	I	0.93	−658
Des4[1]	V	V	—	—	—	S	I	0.78	−656

[1]Des3 and Des4 have the additional buried mutations L147V and A400V, which greatly stabilize the core of the protein and are present in other homologs.

time progressed, it remained constant for Des2 (Figure 3C, Table 3), attesting to the structural integrity of the enzyme's active site in Des2 but not in MMP-9_{Cat}WT after several days of incubation.

Discussion

In this study, we present a novel method for designing protease enzymes that are active and stable to self-cleavage, which is based on the initial identification of the auto-cleavage site and subsequent computational design of non-autocleaving variants. The computational design protocol considered a combination of auto-degradation score, design energy, and the recapitulation of sequence and structural features found in other MMP homologs. Out of four tested variants, one designed variant, Des2, exhibited zero auto-cleavage and retained full catalytic activity up to 7 days of incubation at 37°C, a remarkable stability for a proteolytic enzyme. Furthermore, Des2 bound an active-site MMP-9 inhibitor with the same K_i^{app} as MMP-9_{Cat} WT, indicating that the active site and the enzyme structural properties are unaltered. Furthermore, K_m and k_{cat} values of Des2 were very similar to those of MMP-9_{Cat} WT, proving that the catalytic efficiency of the enzyme was not compromised by the two introduced mutations.

In previous studies, inactive catalytic-site-mutants of MMP-9 were developed, by mutating the catalytic E402 to alanine or asparagine [27,28,33]. Corresponding residues were also mutated in other MMPs [34–38]. These mutants were considerably more stable than the WT MMP constructs and have been utilized to solve crystal structures of various MMPs [28,39]. However, such proteins remained inactive and could not be used in applications such as drug discovery. In contrast, we mutated only the identified self-cleavage site and introduced only two mutations, leaving the catalytic site unaltered. Our modeling with AlphaFold shows that Des2 exhibits an almost identical structure to MMP-9_{Cat} WT overall and especially in the region of the redesigned loop (Figure 2D). Our engineered variant hence offers multiple advantages for studies that require working with MMP-9_{Cat} at high concentrations while preserving its catalytic activity. It is particularly suitable for the discovery of active-site MMP-9 inhibitors that are being conducted in various research laboratories and pharmaceutical companies.

Native enzymes including proteases are intrinsically unstable and frequently difficult to purify and work with. Computational design could be applied to significantly improve enzyme stability. Fleishman and coworkers [40] devised a protocol that allows enzyme stabilization by introducing multiple mutations far from the active site observed in the enzyme evolutionary profile. This strategy, however, achieves enzyme stabilization via multiple mutations and could not be applied to our project where we want to keep MMP-9_{Cat} WT sequence as close to WT as possible. Hence, we developed a different method that combines mass spectroscopy, self-cleavage and stability predictions to remove the self-cleavage site in MMP-9_{Cat} WT.

Table 2. Enzyme kinetic parameters for MMP-9_{Cat} WT and Des2[1]

Variant name	$V_{max} \times 10^{-6}$ moles s^{-1}	K_m (μM)	$k_{cat} \times 10^{-6}$ (s^{-1})	$k_{cat}/K_m \times 10^{-5}$ (μM^{-1} s^{-1})
MMP-9_{Cat} WT	1.54 ± 0.05	8.97 ± 1.45	7.70 ± 0.03	8.6 ± 1.2
Des2	1.33 ± 0.03	7.1 ± 1.0	6.60 ± 0.02	9.4 ± 1.4

[1]All parameters were obtained by fitting the experimental curves shown in Supplementary Figure S4 with equation (2).

Biochemical Journal (2023) 480 1097–1107
https://doi.org/10.1042/BCJ20230139

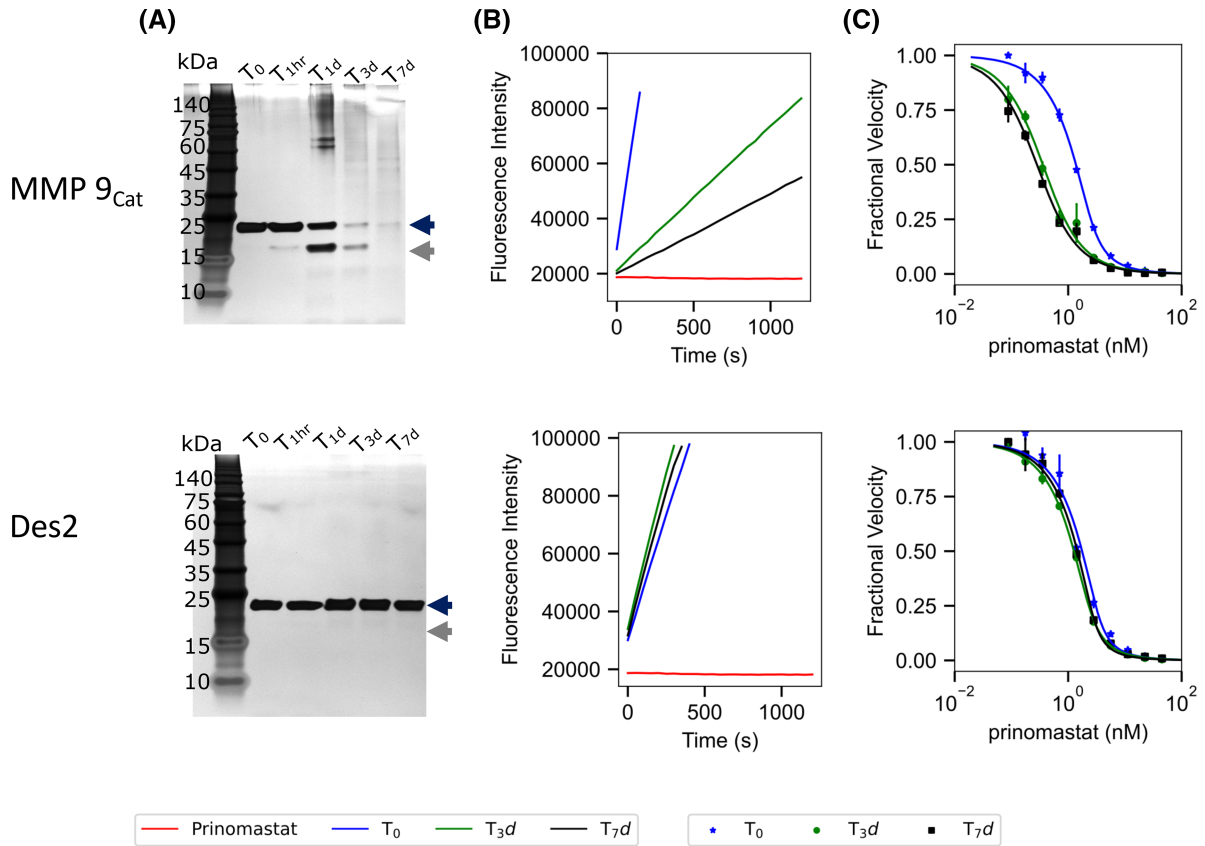

Figure 3. Evaluation of MMP-9_{Cat} WT and Des2 stability and enzyme activity at different time points.
(**A**) Silver-stained SDS–PAGE analysis showing full-length and cleavage products of MMP-9_{Cat} WT (top) and Des2 (bottom) after 37°C at several time intervals, $T = 0$, $T = 1$ h (T_{1hr}), $T = 1$ day (T_{1d}), $T = 3$ days (T_{3d}), and $T = 7$ days (T_{7d}). (**B**) Enzyme activity of MMP-9_{Cat} WT (top) and Des2 (bottom) at T_0, T_{3d}, and T_{7d} using a fluorogenic peptide substrate. Substrate digestion was monitored by the appearance of a fluorescence signal at 395 nm. (**C**) Inhibition of MMP-9_{Cat} WT (top) and Des2 (bottom) at T_0, T_{3d}, and T_{7d} using prinomastat as an inhibitor, using the same fluorogenic substrate as in (**B**). K_i^{app} was determined by fitting the data to Morrison's equation (see equation (1) in Methods) [26].

With our four designs, we tested mutations at positions 414, 415, 417, and 418 (Table 1). Our results show that Des2, the only one with mutations at position 415 had the lowest auto-cleavage activity. Position 415 is exposed to the solvent (Figure 1C), and a mutation here could confer a better auto-cleavage resistance compared with position 418, which is buried. Our best design Des2 recapitulates the sequence of MMP-3 and MMP-10 in the predicted auto-cleavage loop (Figure 2C). Interestingly, in our own experience, MMP-3_{cat} exhibits little auto-cleavage, although this observation was not considered in the design of Des2 sequence. Although

Table 3. Active enzyme concentration and K_i^{app} for prinomastat of MMP-9_{Cat} WT and Des2 at different time points

	T_0		T_1		T_2	
	K_i^{app}, nM[1]	[E], nM[1]	K_i^{app}, nM	[E], nM	K_i^{app}, nM	[E], nM
MMP-9_{Cat} WT	0.30 ± 0.04	2.1 ± 0.2	0.22 ± 0.02	0.27 ± 0.05	0.16 ± 0.03	0.18 ± 0.09
Des2	0.28 ± 0.03	2.9 ± 0.4	0.268 ± 0.003	2.00 ± 0.03	0.18 ± 0.04	2.5 ± 0.3

[1]The parameters were obtained by fitting Figure 3C to equation (1).

PORTLAND PRESS

all four designed MMP-9_{Cat} WT variants were active, only Des2 exhibited stability to self-cleavage. This is consistent with its predicted self-cleavage score (Table 1), which is considerably better than that of MMP-9_{Cat} WT. Des1, Des3, and Des4 exhibit self-cleavage scores only slightly better than that of MMP-9_{Cat} WT. Thus, our results established the range of the Procleave score predictions that produce substantial changes experimentally and could be used to evaluate future self-cleavage-resistant variants.

In conclusion, we computationally designed an MMP-9_{Cat} variant that retained WT-like catalytic activity and binding to a small molecule inhibitor yet abolished undesired auto-degradation property. Our methodology could be applied to the redesign of other enzymes prone to self-cleavage, facilitating future studies of enzyme characterizations, structural determination, and drug design efforts.

Methods

Design of the non-degrading MMP-9_{Cat} variant

For energy calculations, single-position computational mutational scan and multi-position designs were built using Rosetta FastDesign [31], running 20 trajectories per position or multi-position design, and then taking the average score of the best 5. For these calculations, MMP-9_{Cat} crystal structure (PDB: 5TH6) with the pro-domain removed was relaxed using Rosetta FastRelax with SetupMetalsMover [41] and used as the input model in all runs. The backbone co-ordinates were constrained to the input model, and the option use_input_side-chains was used. Only neighbors within 6 Å to any of the eight positions mutated in the mutational scan were allowed to be repacked. The structures of the designed proteins were visually compared with these of the MMP-9 homologs for sequence identity and rotamer conformation similarity.

For the predicted auto-cleavage score, we used the web server procleave developed for substrate-cutting prediction of MMP-9_{Cat} [30], using as input the designed MMP-9_{Cat} sequences.

DNA cloning and mutagenesis

Gene blocks of MMP-9_{Cat} WT and variants Des 3 and Des 4 were purchased from IDT DNA, U.S.A. Primary PCR was carried out to generate the megaprimer, which was used to clone the WT MMP-9 pET28a plasmid using Restriction free Cloning [42]. Mutagenesis primers for Des1 and Des2 were designed and purchased from Integrated DNA Technologies (IDT DNA, U.S.A.) and used to introduce mutations into the WT MMP-9_{cat} gene with the transfer PCR protocol (TPCR) [43]. All primers are summarized in Supplementary Table S1. PCR products were run on a 1% agarose gel to confirm the proper size of the expected PCR product (~6000 bp). PCR products were DpnI digested to eliminate parental bacterial plasmid DNA. pET28a plasmids encoding MMP-9_{Cat} WT and variants were transformed into Top 10 chemically competent cells and plated on liquid broth (LB) agar plates supplemented with 50 μg ml^{-1} antibiotic kanamycin (KAN) and left to incubate at 37°C overnight. Five colonies were picked for each mutant and used to inoculate 5 ml LB media supplemented with 50 μg ml^{-1} of KAN and the cell cultures were grown at 37 °C overnight. The DNA from the grown cultures was isolated using the Mini prep protocol by Geneaid kit (Geneaid, Taiwan) and its concentration was measured using NanoDrop 1000 spectrophotometer. The correct sequences of the MMP-9 mutants were confirmed by Sanger sequencing (HyLabs).

Protein expression

Gene constructs in the pET28a vector were transformed into BL21 (DE3) competent cells for protein expression. The cells were transferred to 1 l of LB supplemented with 50 μg ml^{-1} of KAN. This culture was grown at 30°C until an OD at 600 nm of 0.8–1.2 was reached. Protein expression was then induced with the addition of 1 mM isopropyl-D-1-thiogalactopyranoside (IPTG) and the culture was allowed to grow overnight at 30°C. The following day, the cells were pelleted by centrifuging at 10 000 rpm for 15 min in a SLA1500 or GSA rotor. The pellet was then frozen at −20°C until further processing. Next, pellets were suspended in 30 ml buffer B (25 mM Tris, 0.5 M NaCl, 0.5% v/v triton, pH 8.0) with lysozyme (100 μg ml^{-1}). Finally, the solution was homogenized and incubated at 4°C for 2 h. To wash the inclusion bodies from contaminants, this solution was sonicated (VCX 750 Sonicator cat no. H-1006-2) at 60% amplitude with a large tip probe (13 mm) with 5-s pulses and 5-s rest for 2 min until the color of the solution changed. Next, the sample was centrifuged at 12 500 rpm for 20 min at 4°C with an SS34 rotor. Sonication and centrifugation were repeated three more times. Next, the inclusion bodies were resuspended in 50 ml solubilization buffer C (6 M Urea, 25 mM Tris, pH 8.0). The samples were sonicated again until homogeneity.

Biochemical Journal (2023) 480 1097–1107
https://doi.org/10.1042/BCJ20230139

Protein refolding

Protein refolding was performed on a gravity column at 4°C in the presence of 0.2% zwittergent. First, the MMP-9_{Cat} WT and variants (Des1, Des2, Des3, Des4) were incubated with the Ni^{2+}-NTA agarose affinity column (PureCube cat no. 31103) for an hour. Then, the unbound protein was removed using a wash buffer (6 M Urea, 50 mM Tris, 30 mM NaCl, and 30 mM Imidazole; pH 7.5). Protein refolding of MMP-9_{Cat} WT and variants was achieved by stepwise removal of Urea. First, the column was incubated for 2 hours with Buffer G (4 M Urea, 50 mM Tris, 30 mM NaCl, 5 mM $CaCl_2$, 20 μM $ZnCl_2$, pH7.5), then with Buffer H (2 M Urea, 50 mM Tris, 30 mM NaCl, 5 mM $CaCl_2$, 2 μM $ZnCl_2$, pH 7.5) for another 2 hours, and finally with a Refolding Buffer (50 mM Tris, 30 mM NaCl, 5 mM $CaCl_2$, 20 μM $ZnCl_2$, pH 7.5) overnight. Finally, the proteins were eluted from the column with Elution Buffer (50 mM Tris, 30 mM NaCl, 5 mM $CaCl_2$, and 250 mM imidazole, pH 7.5) and purified using AIEX chromatography (Hitrap Q HP, Cytiva). We further optimized this renaturation protocol by introducing another additive in all of the refolding buffers, a weak inhibitor of MMP-9, AHA [34], at a concentration of 200 mM. The inhibitor was removed using Size exclusion (Hiload 16/60 Superdex 75). Protein concentration was determined by measuring the absorbance at 280 nm using a calculated extinction coefficient of 33 920 M^{-1} cm^{-1}.

Enzymatic activity assay of MMP-9Cat and designs

The proteolytic activity of MMP-9_{Cat} WT, Des1, Des2, Des3, and Des4 was measured using a fluorogenic substrate Dnp-Pro-Leu-Gly-Leu-Trp-Ala-D-Arg-NH2 (Sigma-Aldridge, U.S.A.) in an enzyme activity buffer (50 mM HEPES, 0.1 M NaCl, 10 mM $CaCl_2$, and 0.05% Brij 35, pH = 7.5). Varying concentrations of prinomastat (AG3340, Sigma-Aldridge, U.S.A.) were incubated with MMP-9_{Cat} WT or variant at a final concentration of 2 nM under conditions similar to that described in [23]. Fluorescence resulting from cleavage of the fluorogenic substrate was measured at 395 nm, at least every 10 s for at least 5 min, immediately after adding fluorogenic substrate with irradiation at 325 nm on a Biotek Synergy H1 plate reader (BioTek, Winooski, VT, U.S.A.). Normalized velocities were fitted in MATLAB Curve Fitting Toolbox (MathWorks) to the Morisson equation:

$$\frac{V_i}{V_0} = \frac{(E - I - K_i^{app}) + \sqrt{(E + I + K_i^{app})^2 - 4EI}}{2E} \quad (1)$$

where V_i is the enzyme velocity at inhibitor concentration I, V_0 is the enzyme velocity in the absence of an inhibitor, E is the active enzyme concentration, and K_i^{app} is an apparent inhibitory constant. At least three assays were performed and average values were calculated.

Self-cleavage assay

Samples of pure MMP-9_{Cat} WT and variants at concentration of 0.5 μM were incubated in assay buffer (50 mM Tris, 100 mM NaCl, 5 mM $CaCl_2$, 0.05% Brij35) at 37 °C for several time points (T_0, T_{1hr}, T_{1d}, T_{3d}, T_{7d}) and frozen at −80. Afterward, the auto-cleavage profile of the protein was analyzed on a silver-stained SDS–PAGE gel.

Enzyme kinetics experiments

A twofold serial dilution of MMP Fluorogenic substrate was made with a starting concentration of 100 μM in 150 μl of assay buffer (50 mM Tris pH = 7.5, 100 mM NaCl, 5 mM CaCl and 0.05% Brij) in a 96 well plate. 50 μl of MMP-9_{Cat} WT, was added to a final concentration of 2 nM and final volume of 200 μl reaction buffer. Fluorescence resulting from cleavage of the fluorogenic substrate was immediately measured at 395 nm, at least every 50 s for at least 2 h, at 395 nm on a Biotek Synergy H1 plate reader (BioTek, Winooski, VT, U.S.A.). Velocities were fitted into the Michaelis–Menten equation (2). At least three assays were performed, and average velocities were calculated.

$$V_0 = \frac{V_{max}\,[S]}{K_m + [S]} \quad (2)$$

where V_0 is the initial velocity, V_{max} is the maximum velocity, K_m is the Michaelis–Menten constant, and [S] is the peptide substrate concentration.

LC–MS/MS data analysis

SDS–PAGE gels were thoroughly stained using Coomassie blue and destained using the de-staining solution (H_2O, methanol, and acetic acid in a ratio of 50/40/10 (v/v/v)). MMP-9_{Cat} WT full-length and degradation product bands were excised and chopped into small cubes. The gel pieces were destained (25 mM Tris–HCl, pH 8.0 containing and acetonitrile (ACN)), treated with 10 mM Dithiothreitol (DTT) (Sigma Chem. Co.) and 55 mM iodoacetamide (Sigma Chem. Co.) and then digested with trypsin (Mass Spectrometry grade, from Promega Corp., Madison, WI, U.S.A.) overnight. The released peptides were extracted, desalted, and eluted using 80% ACN and 0.1% formic acid; 0.25 µg of eluted peptides was used for each sample to obtain the raw data. Mass spectrometry raw data were processed and searched using the Trans-Proteomic Pipeline (TPP) 6.0.0 'OmegaBlock' [44]. Searches were performed using Comet (2020.01 rev. 1) and high-resolution settings. They include 'semi-tryptic' cleavage specificity and oxidation of methionine and protein N-terminal acetylation as variable modifications. All searches were conducted against *E. coli* protein sequences downloaded from UniProt supplemented with the sequence of MMP-9_{Cat}. Following the database search the putative self-cleavage sites generated by MMP-9 were mapped to the sequence using PeptideMatcher script and the P1 positions of cleavage sites were assigned with a value calculated from integrated MS/MS count of all the corresponding peptides.

Data Availability

Analyzed Mass Spectroscopy data is uploaded as Supplementary data while the raw data are available via ProteomeXchange with identifier PXD041767.

Competing Interests

The authors declare that there are no competing interests associated with the manuscript.

Funding

J.S.M. is supported by the US-Israel Binational Science Foundation (BSF) 2017207, NIH R01CA258274, Israel Cancer Research Foundation (ICRF), Israel Science Foundation (3486/20), and the U. of Toronto/HUJI research alliance in protein engineering.

CRediT Author Contribution

Alessandro Bonadio: Conceptualization, Software, Formal analysis, Methodology, Writing — original draft, Writing — review and editing. **Solomon Oguche**: Validation, Investigation, Visualization, Writing — review and editing. **Tali Lavy**: Formal analysis. **Oded Kleifeld**: Formal analysis, Writing — review and editing. **Julia Shifman**: Formal analysis, Supervision, Resources, Funding acquisition, Writing — original draft, Project administration, Writing — review and editing.

Abbreviations

ACN, acetonitrile; AHA, acetohydroxamic acid; AIEX, anion exchange; KAN, kanamycin; LB, liquid broth; MMP-9, matrix metalloproteinase-9; MMP-9_{Cat}, catalytic domain of MMP-9; MMPs, matrix metalloproteinases.

References

1 Cauwe, B., Den Steen, P.E.V. and Opdenakker, G. (2007) The biochemical, biological, and pathological kaleidoscope of cell surface substrates processed by matrix metalloproteinases. *Crit. Rev. Biochem. Mol. Biol.* **42**, 113–185 https://doi.org/10.1080/10409230701340019
2 Christensen, J. and Shastri, V.P. (2015) Matrix-metalloproteinase-9 is cleaved and activated by Cathepsin K. *BMC Res. Notes* **8**, 1–8 https://doi.org/10.1186/s13104-015-1284-8
3 Tallant, C., Marrero, A. and Gomis-Rüth, F.X. (2010) Matrix metalloproteinases: fold and function of their catalytic domains. *Biochim. Biophys. Acta - Mol. Cell Res.* **1803**, 20–28 https://doi.org/10.1016/j.bbamcr.2009.04.003
4 Conlon, G.A. and Murray, G.I. (2019) Recent advances in understanding the roles of matrix metalloproteinases in tumour invasion and metastasis. *J. Pathol.* **247**, 629–640 https://doi.org/10.1002/path.5225
5 Raeeszadeh-Sarmazdeh, M., Do, L.D. and Hritz, B.G. (2020) Metalloproteinases and their inhibitors: potential for the development of new therapeutics. *Cells* **9**, 1313 https://doi.org/10.3390/CELLS9051313

Biochemical Journal (2023) **480** 1097–1107
https://doi.org/10.1042/BCJ20230139

6 Rydlova, M., Holubec, L., Ludvikova, M., Kalfert, D., Franekova, J., Povysil, C. et al. (2008) Biological activity and clinical implications of the matrix metalloproteinases. *Anticancer Res.* **28**, 1389–1397 PMID: 18505085

7 Decock, J., Thirkettle, S., Wagstaff, L. and Edwards, D.R. (2011) Matrix metalloproteinases: protective roles in cancer. *J. Cell. Mol. Med.* **15**, 1254–1265 https://doi.org/10.1111/j.1582-4934.2011.01302.x

8 Folgueras, A.R., Pendás, A.M., Sánchez, L.M. and López-Otín, C. (2004) Matrix metalloproteinases in cancer: from new functions to improved inhibition. *Int. J. Dev. Biol.* **48**, 411–424 https://doi.org/10.1387/ijdb.041811af

9 López-Otín, C. and Matrisian, L.M. (2007) Emerging roles of proteases in tumour suppression. *Nat. Rev. Cancer* **7**, 800–808 https://doi.org/10.1038/nrc2228

10 Sarper, M., Allen, M.D., Gomm, J., Haywood, L., Decock, J., Thirkettle, S. et al. (2017) Loss of MMP-8 in ductal carcinoma in situ (DCIS)-associated myoepithelial cells contributes to tumour promotion through altered adhesive and proteolytic function. *Breast Cancer Res.* **19**, 33 https://doi.org/10.1186/s13058-017-0822-9

11 Coussens, L.M., Fingleton, B. and Matrisian, L.M. (2002) Matrix metalloproteinase inhibitors and cancer—trials and tribulations. *Science* **295**, 2387–2392 https://doi.org/10.1126/science.1067100

12 Winer, A., Adams, S. and Mignatti, P. (2018) Matrix metalloproteinase inhibitors in cancer therapy: turning past failures into future successes. *Mol. Cancer Ther.* **17**, 1147–1155 https://doi.org/10.1158/1535-7163.MCT-17-0646

13 Cathcart, J.M. and Cao, J. (2015) MMP inhibitors: past, present and future. *Front. Biosci. - Landmark* **20**, 1164–1178 https://doi.org/10.2741/4365

14 Fischer, T. and Riedl, R. (2019) Inhibitory antibodies designed for matrix metalloproteinase modulation. *Molecules* **24**, 2265 https://doi.org/10.3390/MOLECULES24122265

15 Levin, M., Udi, Y., Solomonov, I. and Sagi, I. (2017) Next generation matrix metalloproteinase inhibitors — novel strategies bring new prospects. *Biochim. Biophys. Acta - Mol. Cell Res.* **1864**, 1927–1939 https://doi.org/10.1016/j.bbamcr.2017.06.009

16 Appleby, T.C., Greenstein, A.E., Hung, M., Liclican, A., Velasquez, M., Villasenor, A.G. et al. (2017) Biochemical characterization and structure determination of a potent, selective antibody inhibitor of human MMP9. *J. Biol. Chem.* **292**, 6810–6820 https://doi.org/10.1074/jbc.M116.760579

17 Shah, M.A., Yanez Ruiz, E.P., Bodoky, G., Starodub, A., Cunningham, D., Yip, D. et al. (2019) A phase III, randomized, double-blind, placebo-controlled study to evaluate the efficacy and safety of andecaliximab combined with mFOLFOX6 as first-line treatment in patients with advanced gastric or gastroesophageal junction adenocarcinoma (GAMMA-1). *J. Clin. Oncol.* **37**, 4 https://doi.org/10.1200/jco.2019.37.4_suppl.4

18 Udi, Y., Grossman, M., Solomonov, I., Dym, O., Rozenberg, H., Moreno, V. et al. (2015) Inhibition mechanism of membrane metalloprotease by an exosite-swiveling conformational antibody. *Structure* **23**, 104–115 https://doi.org/10.1016/j.str.2014.10.012

19 Nguyen, T.T., Ding, D., Wolter, W.R., Pérez, R.L., Champion, M.M., Mahasenan, K.V. et al. (2018) Validation of matrix metalloproteinase-9 (MMP-9) as a novel target for treatment of diabetic foot ulcers in humans and discovery of a potent and selective small-molecule MMP-9 inhibitor that accelerates healing. *J. Med. Chem.* **61**, 8825–8837 https://doi.org/10.1021/acs.jmedchem.8b01005

20 Bahudhanapati, H., Zhang, Y., Sidhu, S.S. and Brew, K. (2011) Phage display of tissue inhibitor of metalloproteinases-2 (TIMP-2): identification of selective inhibitors of collagenase-1 (metalloproteinase 1 (MMP-1)). *J. Biol. Chem.* **286**, 31761–31770 https://doi.org/10.1074/jbc.M111.253328

21 Sharabi, O., Shirian, J., Grossman, M., Lebendiker, M., Sagi, I. and Shifman, J. (2014) Affinity- and specificity-enhancing mutations are frequent in multispecific interactions between TIMP2 and MMPs. *PLoS One* **9**, e93712 https://doi.org/10.1371/journal.pone.0093712

22 Shirian, J., Arkadash, V., Cohen, I., Sapir, T., Radisky, E.S., Papo, N. et al. (2018) Converting a broad matrix metalloproteinase family inhibitor into a specific inhibitor of MMP-9 and MMP-14. *FEBS Lett.* **592**, 1122–1134 https://doi.org/10.1002/1873-3468.13016

23 Arkadash, V., Yosef, G., Shirian, J., Cohen, I., Horev, Y., Grossman, M. et al. (2017) Development of high affinity and high specificity inhibitors of matrix metalloproteinase 14 through computational design and directed evolution. *J. Biol. Chem.* **292**, 3481–3495 https://doi.org/10.1074/jbc.M116.756718

24 Arkadash, V., Radisky, E.S. and Papo, N. (2018) Combinatorial engineering of N-TIMP2 variants that selectively inhibit MMP9 and MMP14 function in the cell. *Oncotarget* **9**, 32036 https://doi.org/10.18632/ONCOTARGET.25885

25 Yano, H., Nishimiya, D., Kawaguchi, Y., Tamura, M. and Hashimoto, R. (2020) Discovery of potent and specific inhibitors targeting the active site of MMP-9 from the engineered SPINK2 library. *PLoS One* **15**, e0244656 https://doi.org/10.1371/journal.pone.0244656

26 Doucet, A. and Overall, C.M. (2011) Broad coverage identification of multiple proteolytic cleavage site sequences in complex high molecular weight proteins using quantitative proteomics as a complement to Edman sequencing. *Mol. Cell. Proteomics* **10**, M110.003533 https://doi.org/10.1074/MCP.M110.003533

27 Tranchant, I., Vera, L., Czarny, B., Amoura, M., Cassar, E., Beau, F. et al. (2014) Halogen bonding controls selectivity of FRET substrate probes for MMP-9. *Chem. Biol.* **21**, 408–413 https://doi.org/10.1016/j.chembiol.2014.01.008

28 Tochowicz, A., Maskos, K., Huber, R., Oltenfreiter, R., Dive, V., Yiotakis, A. et al. (2007) Crystal structures of MMP-9 complexes with five inhibitors: contribution of the flexible Arg424 side-chain to selectivity. *J. Mol. Biol.* **371**, 989–1006 https://doi.org/10.1016/j.jmb.2007.05.068

29 Rawlings, N.D., Waller, M., Barrett, A.J. and Bateman, A. (2014) MEROPS: the database of proteolytic enzymes, their substrates and inhibitors. *Nucleic Acids Res.* **42**, D503–D509 https://doi.org/10.1093/nar/gkt953

30 Li, F., Leier, A., Liu, Q., Wang, Y., Xiang, D., Akutsu, T. et al. (2020) Procleave: predicting protease-specific substrate cleavage sites by combining sequence and structural information. *Genom. Proteom. Bioinform.* **18**, 52–64 https://doi.org/10.1016/j.gpb.2019.08.002

31 Nivón, L.G., Moretti, R. and Baker, D. (2013) A Pareto-optimal refinement method for protein design scaffolds. *PLoS One* **8**, e59004 https://doi.org/10.1371/JOURNAL.PONE.0059004

32 Morrison, J.F. (1969) Kinetics of the reversible inhibition of enzyme-catalysed reactions by tight-binding inhibitors. *Biochim. Biophys. Acta* **185**, 269–286 https://doi.org/10.1016/0005-2744(69)90420-3

33 Bailón, E., Aguilera-Montilla, N., Gutiérrez-González, A., Ugarte-Berzal, E., Van den Steen, P.E., Opdenakker, G. et al. (2018) A catalytically inactive gelatinase B/MMP-9 mutant impairs homing of chronic lymphocytic leukemia cells by altering migration regulatory pathways. *Biochem. Biophys. Res. Commun.* **495**, 124–130 https://doi.org/10.1016/j.bbrc.2017.10.129

34 Gutiérrez-Fernández, A., Soria-Valles, C., Osorio, F.G., Gutiérrez-Abril, J., Garabaya, C., Aguirre, A. et al. (2015) Loss of MT 1- MMP causes cell senescence and nuclear defects which can be reversed by retinoic acid. *EMBO J.* **34**, 1875–1888 https://doi.org/10.15252/embj.201490594

35 Cha, J. and Auld, D.S. (1997) Site-directed mutagenesis of the active site glutamate in human matrilysin: investigation of its role in catalysis. *Biochemistry* **36**, 16019–16024 https://doi.org/10.1021/bi972223g

36 Kleifeld, O., Doucet, A., Auf Dem Keller, U., Prudova, A., Schilling, O., Kainthan, R.K. et al. (2010) Isotopic labeling of terminal amines in complex samples identifies protein N-termini and protease cleavage products. *Nat. Biotechnol.* **28**, 281–288 https://doi.org/10.1038/nbt.1611
37 Paladini, R.D., Wei, G., Kundu, A., Zhao, Q., Bookbinder, L.H., Keller, G.A. et al. (2013) Mutations in the catalytic domain of human matrix metalloproteinase-1 (MMP-1) that allow for regulated activity through the use of Ca^{2+}. *J. Biol. Chem.* **288**, 6629–6639 https://doi.org/10.1074/jbc.M112.364729
38 Valtanen, H., Lehti, K., Lohi, J. and Keski-Oja, J. (2000) Expression and purification of soluble and inactive mutant forms of membrane type 1 matrix metalloproteinase. *Protein Expr. Purif.* **19**, 66–73 https://doi.org/10.1006/prep.2000.1216
39 Rowsell, S., Hawtin, P., Minshull, C.A., Jepson, H., Brockbank, S.M.V., Barratt, D.G. et al. (2002) Crystal structure of human MMP9 in complex with a reverse hydroxamate inhibitor. *J. Mol. Biol.* **319**, 173–181 https://doi.org/10.1016/S0022-2836(02)00262-0
40 Goldenzweig, A., Goldsmith, M., Hill, S.E., Gertman, O., Laurino, P., Ashani, Y. et al. (2016) Automated structure- and sequence-based design of proteins for high bacterial expression and stability. *Mol. Cell* **63**, 337–346 https://doi.org/10.1016/j.molcel.2016.06.012
41 Mulligan, V.K., Workman, S., Sun, T., Rettie, S., Li, X., Worrall, L.J. et al. (2021) Computationally designed peptide macrocycle inhibitors of New Delhi metallo-β-lactamase 1. *Proc. Natl Acad. Sci. U.S.A.* **118**, e2012800118 https://doi.org/10.1073/pnas.2012800118
42 Bond, S.R. and Naus, C.C. (2012) RF-Cloning.org: an online tool for the design of restriction-free cloning projects. *Nucleic Acids Res.* **40**, W209 https://doi.org/10.1093/nar/gks396
43 Erijman, A., Shifman, J.M. and Peleg, Y. (2014) A single-tube assembly of DNA using the transfer-PCR (TPCR) platform. *Methods Mol. Biol.* **1116**, 89–101 https://doi.org/10.1007/978-1-62703-764-8_7
44 Deutsch, E.W., Mendoza, L., Shteynberg, D., Farrah, T., Lam, H., Tasman, N. et al. (2010) A guided tour of the trans-proteomic pipeline. *Proteomics* **10**, 1150–1159 https://doi.org/10.1002/pmic.200900375